Microdiffraction: X-Rays As A Probe To Reveal Flux Divergences In Interconnects

R. Spolenak[1], N. Tamura[2], and J. R. Patel[2,3]

[1]*Lab. for Nanometallurgy, Dept. of Materials, ETH Zurich, 8093 Zurich, Switzerland*
[2]*Advanced Light Source, Lawrence Berkeley National Laboratory, Berkeley, CA 94720, USA*
[3]*Department of Materials Science & Engineering, Stanford University, Stanford, CA 94305, USA*

Abstract. Most reliability issues in interconnect systems occur at a local scale and many of them include the local build-up of stresses. Typical failure mechanisms are electromigration and stress voiding in interconnect lines and fatigue in surface acoustic wave devices. Thus a local probe is required for the investigation of these phenomena. In this paper the application of the Laue microdiffraction technique to investigate flux divergences in interconnect systems will be described. The deviatoric strain tensor of single grains can be correlated with the local microstructure, orientation and defect density. Especially the latter led to recent results about the correlation of stress build-up and orientation in Cu lines and electromigration-induced grain rotation in Cu and Al lines.

Keywords: copper, electromigration, Laue microdiffraction, critical product, surface diffusion.
PACS: 61.10.Nz, 62.25.+g, 66.30.Qa, 68.55.-a, 68.55.Ln

INTRODUCTION

Electromigration has been a reliability issue for microelectronics for several decades[1-4]. The change in technology from subtractive aluminum back-end processes to damascene copper technology has alleviated the issue, but different materials issues have arisen. With the introduction of low-k dielectrics and thus the absence of a mechanically restraining material around the conductor lines, additional electromigration issues are to be anticipated.

X-ray Laue microdiffraction has recently been used to study electromigration phenomena[5-8]. Novel insight has been gained by monitoring the size and orientation of single Laue spots as a function of time during an *in situ* electromigration experiment. Peak broadening and peak splitting was observed that led to the conclusion that the electromigrated atoms were incorporated in newly formed small-angle grain boundaries oriented along the current flow. The monitoring of the evolution of stresses proved to be extremely difficult due to the large inhomogeneities already preexisting in the line[9,10]. Unlike other studies where broader beams had been used[11], a clear stress gradient could not be observed.

In this study we focused on an *in situ* study of copper damascene lines by monitoring the local deviatoric stress states as a function of time, current density and

current direction. The aim of this study was to identify the locations of flux divergence by identifying grains that showed strong changes in stress upon current reversal.

EXPERIMENTAL

The samples were prepared in a standard Cu damascene technique with a tantalum diffusion barrier. The line thickness was 1 micron, their width 0.8 and 2 microns and the diffusion barrier was 50 nm thick. The dielectric was PE-TEOS and the cap layer consisted of 200 nm PECVD SiN_x. Fig. 1 shows the sample as a schematic in cross-section and the corresponding FIB image. The lines were 10 , 20, 30, 50 and 100 microns long all connected by wide 200 nm thick tantalum segments as indicated in Fig.1. The samples were similar to the geometry suggested by Blech *et al.*[3,12].

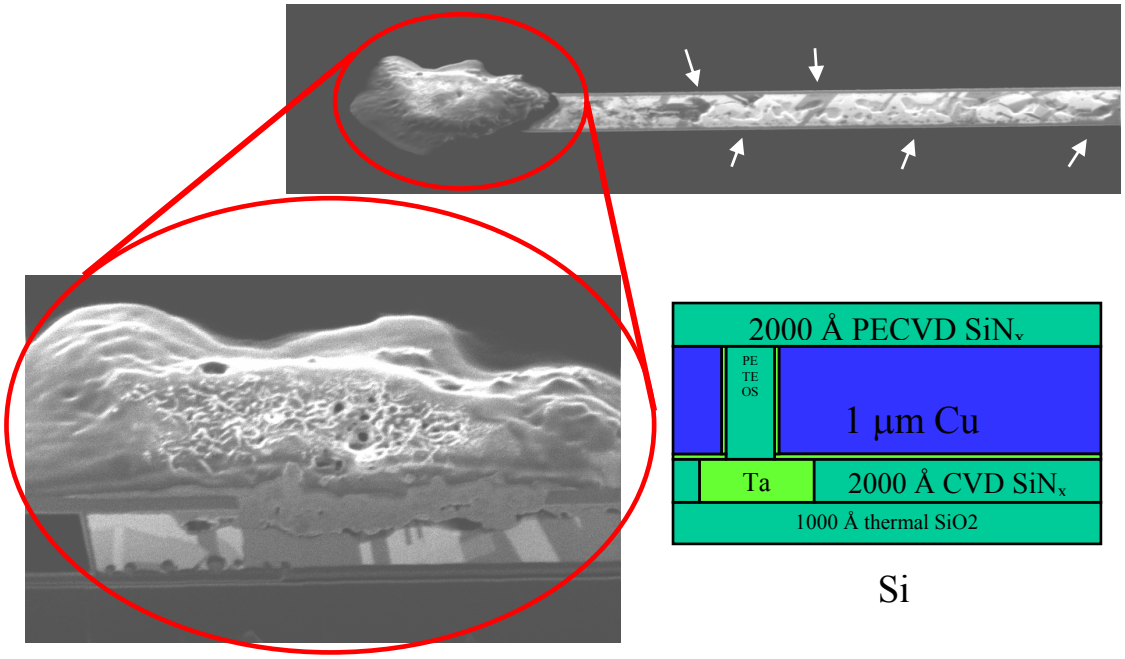

FIGURE 1. Electromigration damage in a Blech type, 2 micron wide, Cu damascene line, the lower right part shows a schemativ of the crosssection visible in the lower left part, white arrows indicate surface voids. The hillock on the top left has cracked the passivation at test temperature and has consequently oxidized.

In situ electromigration tests were performed under a focused Laue X-ray microbeam at beamline 7.3.3 of the Advanced Light Source (ALS) of the Lawrence Berkeley Lab (LBL). The current densities ranged from 0.5 MA/cm^2 to 1.5 MA/cm^2 and were incremented and reversed during the experiment. The experiments were carried out at 223°C at air. When the hillocks forming broke the passivation, they were immediately oxidized as indicated in the inset of Fig. 1. The samples were characterized after the tests by focused ion beam (FIB) and optical microscopy. X-ray microdiffraction as described by Tamura *et al.*[13,14] was used during the electromigration test to determine orientation and five components of the strain tensor.

Strain maps were acquired before the test and every time after the current condition was changed and the resistivity of the line had stabilized.

RESULTS

Fig. 2 shows and FIB micrograph at 45° of a 50 micron long line after the test. The SiN_x layer had been removed by a selective insulator etch (XeF_2) before imaging. Fig. 2 shows a near bamboo microstructure of the line. Several twins can be observed and the surface shows small voids all along the line. The furthest left of line is marked by a large hillock that had been oxidized in air after the passivation had been cracked by the hillock.

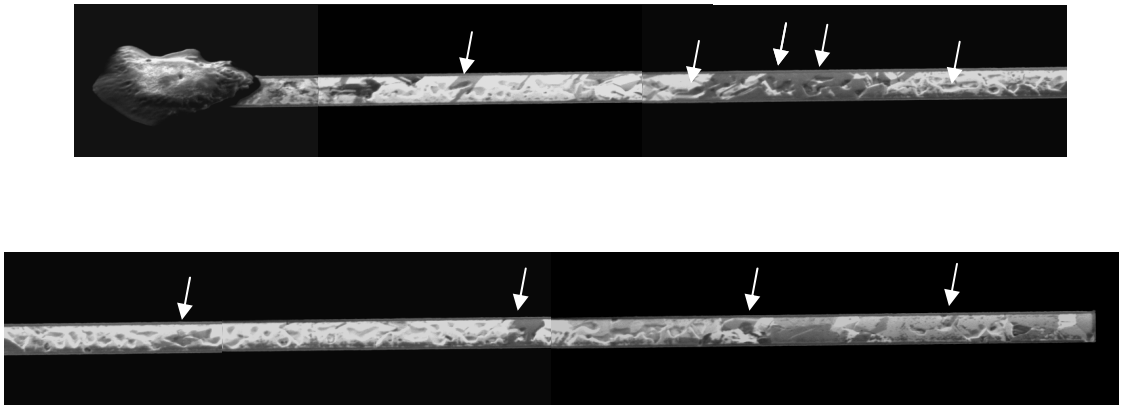

FIGURE 2. Damage at the top interface can be observed throughout the entire line. The line is 2 microns wide and 50 microns long and imaged at an angle of 45°. Voids are indicated by arrows.

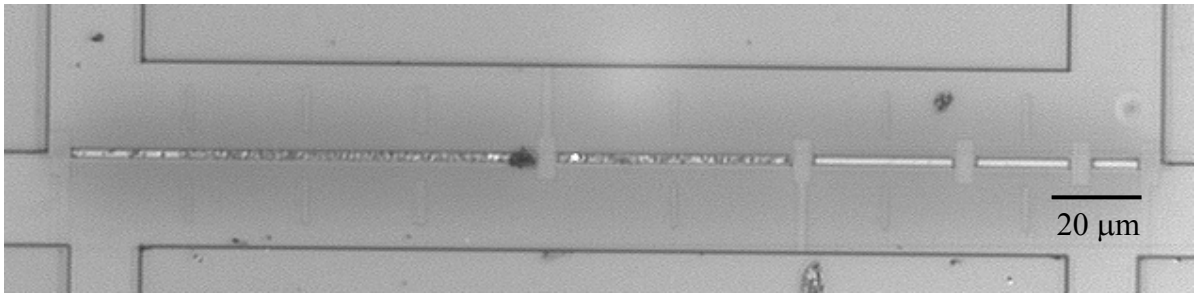

FIGURE 3. Optical micrograph of a series of damascene Blech segements of increasing length. Only the two segments to the left show damage.

Fig. 3 shows an optical view of the entire structure after an electromigration test at 1 MA/cm^2 current density. Only the two longest segments of 50 and 100 microns of a 2 micron wide structure show damage. The segments of 10, 20 and 30 microns length show no damage at all. The critical product $(jl)_c$ for this experiment would then amount to [3,12,15-18]:

$$3000 \text{ A/cm} < (jl)_c < 5000 \text{ A/cm} \qquad (1)$$

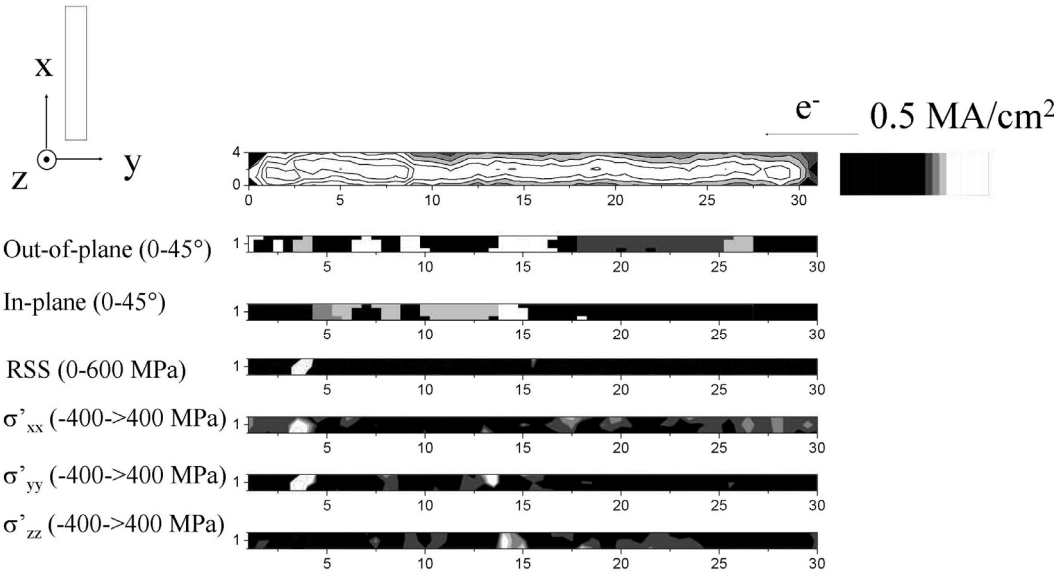

FIGURE 4. Orientation and stress maps of a 0.8 μm wide, 30 μm long damascene Blech segment during an electromigration test. In the out of plane map black areas are (111) oriented, white are (115) oriented and grey areas are (5 7 13) oriented. The range of the black to white contrast is indicated in brackets beside the maps.

Fig. 4 shows microdiffraction results briefly after the application of the current. The top line shows the summed intensity of the Laue images. It is apparent that the line is in the center of the map during the whole experiment. The intensity decrease from the left to the right is due the decrease in flux by the synchrotron, which needed to be refilled with electrons every four hours. The next two maps characterize the orientation of the 30 micron long line. The left part shows mostly (111) orientation out of plane with some (115) oriented twin segments, whereas the left of the line shows a doubly twinned orientation of (5 7 13) out of plane. The resolved shear stress map (RSS) shows that the stresses vary significantly from grain to grain. Similar effects are visible in the three maps of deviatoric stress states.

Fig. 5 shows the changes in stress states as caused by increases in current and current reversal. This strategy was adopted to visualize the flux divergences associated with the electromigration process. The areas in the maps where strong changes in stresses were observed are indicated by black lines. They seem to be correlated with the following grain boundaries: a grain boundary between a (111) oriented grain and a twinned grain (115), a boundary between two (115) oriented grains and a boundary between a (115) and a (5 7 13) oriented grain. This can be deduced from a combination of the in plane and out of plane orientation maps.

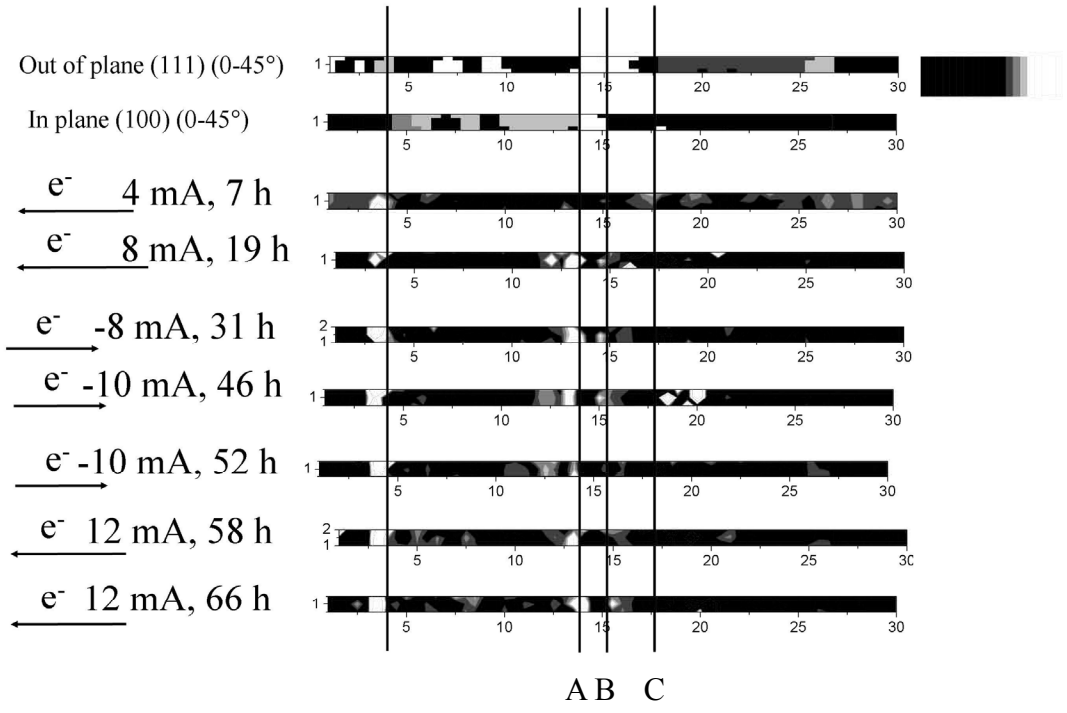

FIGURE 5. The evolution of stresses in a damascene Blech segment as a function of time, current density and current direction. The locations of local stress evolution are correlated with the crystallographic orientation of single grains and marked by black lines. The black line on the furthest left is a reference to align the maps. Label A marks a boundary between a (111) grain and a (115) grain. Label B marks a boundary between two (115) grains with different in plane orientation and label C marks a boundary between a (115) grain and a (5 7 13) grain.

DISCUSSION

We consider the top surface to be the dominating diffusion path in our experiment, which has also been confirmed by other groups[19,20]. In this paper, one can find evidence in Fig. 1, where voiding at the top surface can be observed. The focus of this paper is now to determine, which the flux divergences are that can be found in Cu damascene structures in addition to the trivial ones (start and end of the Blech segments).

Fig. 5 shows some examples of flux divergences that had been identified by ramping the current density and current reversal and observing the sites that exhibited the strongest change in stress. One location on the left always showed the same high stress state, which however did not change and was therefore not considered a flux divergence. Three general types of flux divergence were observed: grain boundaries between (111) and (115) grains (oriented out of plane), grain boundaries between (115) and (115) grains, and grain boundaries between (115) and (5 7 13) grains.

Fig. 6 provides an interesting insight into the respective surfaces. The (111) surface is fairly isotropic, whereas the (115) shows a strong in plane anisotropy. The [-1 1 0]

direction in plane, in the latter case is the fastest direction for surface diffusion. This anisotropy, which can also be expected for (5 7 13) surfaces can explain all scenarios mentioned above. In case A, a (111) and a (115) grain neighbor each other. The degree of flux divergence then depends on the orientation of the (115) grain relative to the line direction. In case B, two neighboring (115) grains, it depends on the relative orientation between the two grains, however. If they were perfectly aligned, the flux divergence would disappear, at normal angles of the respective [-1 1 0] directions the flux divergence would be maximized. Similar arguments can be made for case C, a boundary between (115) and (5 7 13).

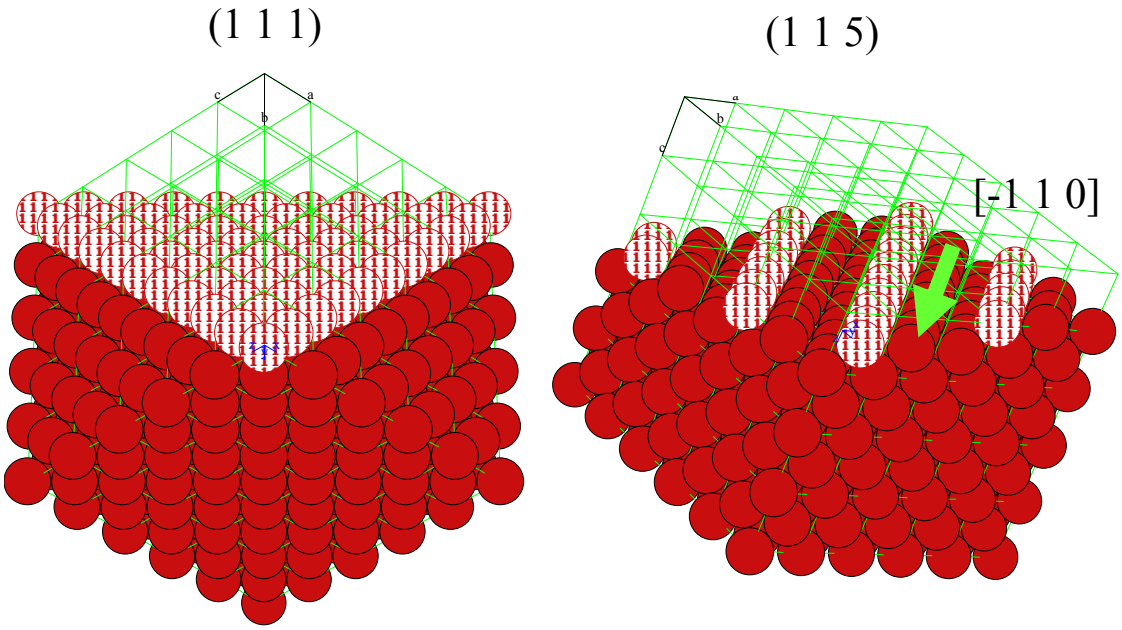

FIGURE 6. Schematic of (111) and (115) surfaces without reconstruction. The (115) surface exhibits a strong in plane anisotropy.

Having identified the flux divergences, the next question would be, which stress states are possible. Fig. 7 gives an answer to this question. Being blocked at the grain boundary at the flux divergence atoms can be incorporated a) in the grain boundary itself, b) in the sidewalls and c) at the top surface itself. All these scenarios lead to different stress states which in principle could be identified by Laue microdiffraction, however, require a more systematic study. One should bare in mind that so far Laue microdiffraction can only measure the deviatoric components of stress. In this case the hydrostatic component would be quite sensitive to flux divergences.

Budiman *et al.*[5,6] recently observed in Cu damascene lines that in grains close to the cathode end peak splitting as well as peak broadening was observed. Both effects were oriented normal to the line direction. This is indicative of and incorporation of atoms either at the side wall or at the top surface, but not in the grain boundary itself. In the case of peak splitting a dislocation mechanism has also be involved to account for the absorption of atoms as peak splitting is evidence for the formation of a small angle tilt boundary.

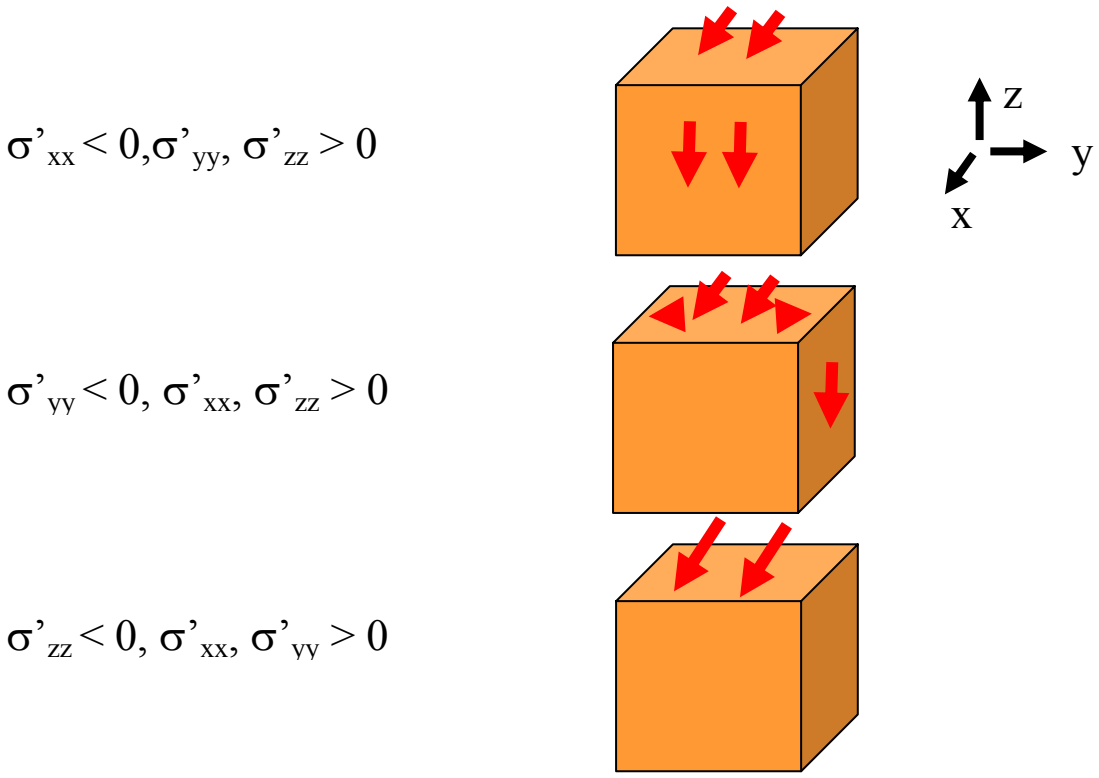

FIGURE 7. Possible flux divergences for a surface diffusion path. In the top scenario atoms are incorporated into the grain boundary whose normal direction is parallel to the electromigration flow; the resulting stress state is compressive along the line direction. In the second scenario this grain boundary is blocked and atoms are incorporated in the side walls. Here, the resulting stress state is compressive across the line direction. In the bottom scenario, atoms are incorporated directly at the flux divergence and the resulting stress state is compressive out of plane.

The last point to discuss is Fig. 3, where a critical product can be determined. The critical product lies between 3000 and 5000 A/cm, which is in general agreement with other observations[21,22]. It also critically depends on the fracture toughness and thickness of the passivation layer as it determines the critical stress that can be built up in such a structure. This in turn determines critical stress gradient needed to calculate the critical product. The fracture of the passivation layer can be seen in Figs. 1, 2 and 3 and has caused the copper hillock to oxidize, as the experiments were carried out at ambient air.

CONCLUSIONS

The following points have been shown in this paper. A critical product for Cu damascene lines has been identified through Blech type structures. The main diffusion path in these damascene structures has been identified as the interface between the top of the line and the SiN_x passivation layer. Flux divergences as identified by Laue microdiffraction have been correlated to the microstructure of the sample and been explained by anisotropic surface/interface diffusion depending on the crystal

orientation. The most important incorporation surfaces of the arriving atoms are the top surface itself or the sidewalls.

The following conclusions can be drawn from these observations: a) the control of the Cu microstructure (out of plane as well as in plane) is extremely important and should be optimized by process conditions during fabrication, b) performing the experiments described above in a time resolved way, one could in principal determine the surface diffusivities of Cu damascene structures. The latter would be quite valuable as input data for lifetime modeling.

The control of the microstructure could in principal be also achieved by novel post deposition ion bombardment methods[23,24], where selective grain growth is caused by ion bombardment.

ACKNOWLEDGMENTS

The authors acknowledge the SSRL laboratory at Bell Labs Lucent Technologies for the fabrication of damascene samples. The Advanced Light Source (ALS) is supported by the Director, Office of Science, Office of Basic Energy Sciences, Materials Sciences Division, of the U.S. Department of Energy under Contract No. DE-AC03-76SF00098 at Lawrence Berkeley National Laboratory.

REFERENCES

1. E. Arzt, O. Kraft, R. Spolenak, and Y.-C. Joo, *Z. Metallkd.* **87**, 934 (1996).
2. J. R. Black, *IEEE Tr. E. D.* **ED-16**, 338 (1969).
3. I. A. Blech, *J. Appl. Phys.* **47** (4), 1203 (1976).
4. A. R. Grone, *J. Phys. Chem. Solids* **20**, pp. 88 (1961).
5. A. S. Budiman, N. Tamura, B. C. Valek, K. Gadre, J. Maiz, R. Spolenak, W. A. Caldwell, W. D. Nix, and J. R. Patel, in *Materials, Technology and Reliability for Advanced Interconnects and Low-K Dielectrics-2004* (2004), Vol. 812, pp. 345.
6. A. S. Budiman, N. Tamura, B. C. Valek, K. Gadre, J. Maiz, R. Spolenak, W. D. Nix, and J. R. Patel, *to be submitted to Appl. Phys. Lett.* (2005).
7. B. C. Valek, J. C. Bravman, N. Tamura, A. A. MacDowell, R. S. Celestre, H. A. Padmore, R. Spolenak, W. L. Brown, B. W. Batterman, and J. R. Patel, *Applied Physics Letters* **81** (22), 4168 (2002).
8. B. C. Valek, N. Tamura, R. Spolenak, W. A. Caldwell, A. A. MacDowell, R. S. Celestre, H. A. Padmore, J. C. Braman, B. W. Batterman, W. D. Nix, and J. R. Patel, *Journal of Applied Physics* **94** (6), 3757 (2003).
9. R. Spolenak, W. L. Brown, N. Tamura, A. A. MacDowell, R. S. Celestre, H. A. Padmore, B. Valek, J. C. Bravman, T. Marieb, H. Fujimoto, B. W. Batterman, and J. R. Patel, *Physical Review Letters* **90** (9) (2003).
10. R. Spolenak, N. Tamura, B. C. Valek, A. A. MacDowell, R. S. Celestre, H. A. Padmore, W. L. Brown, T. Marieb, and J. R. Patel, in *Stress-Induced Phenomena in Metallization* (2002), Vol. 612, pp. 217.
11. P.-C. Wang, G. S. Cargill III, I. C. Noyan, and C.-K. Hu, *Appl. Phys. Letters* **72** (11), 1296 (1998).
12. I. A. Blech and K. L. Tai, *Appl. Phys. Lett.* **30** (8), 387 (1977).
13. N. Tamura, R. S. Celestre, A. A. MacDowell, H. A. Padmore, R. Spolenak, B. C. Valek, N. M. Chang, A. Manceau, and J. R. Patel, *Review of Scientific Instruments* **73** (3), 1369 (2002).
14. N. Tamura, A. A. MacDowell, R. Spolenak, B. C. Valek, J. C. Bravman, W. L. Brown, R. S. Celestre, H. A. Padmore, B. W. Batterman, and J. R. Patel, *Journal of Synchrotron Radiation* **10**, 137 (2003).
15. J. J. Clement and C. V. Thompson, *J. Appl. Phys.* **78** (2), 900 (1995).
16. R. Kirchheim, *Acta metall. mater.* **40** (2), 309 (1992).
17. M.A. Korhonen, P. Børgesen, K. N. Tu, and C.-Y. Li, *J. Appl. Phys.* **73** (8), 3790 (1993).
18. J. R. Kraayeveld, A. H. Verbruggen, and A. W.-J. Willemsen, *Appl. Phys. Lett.* **67** (9), 1226 (1995).
19. M. H. Lin, Y. L. Lin, K. P. Chang, K. C. Su, and T. H. Wang, **45** (7-8), 1061 (2005).
20. K. D. Lee and P. S. Ho, **4** (2), 237 (2004).
21. E. T. Ogawa, K. D. Lee, V. A. Blaschke, and P. S. Ho, **51** (4), 403 (2002).
22. R. Frankovic and G. H. Bernstein, **43** (12), 2233 (1996).

23. R. Spolenak, L. Sauter, and Eberl. C., *Scripta Materialia* **53**, 1291 (2005).
24. S. Olliges, P. Gruber, H. D. Carstanjen, and R. Spolenak, *in preparation* (2005).